

Finite Element Study of Hard and Soft Inclusions in Hard/soft Matrix

Michal Kráčalik *

Untere Hauptstraße 48/5, 2424 Zurndorf, Austria

Abstract: Hard inclusions in the soft matrix are common in metal matrix composites. On the other hand, soft inclusions in the hard matrix can be found for instance in plastics like acrylonitrile-butadiene-styrene (ABS). This work focuses on the finite element study of hard inclusions in the soft matrix and soft inclusions in the hard matrix. Equivalent von-Mises Stress and Equivalent plastic strain are evaluated. Hard inclusions in the soft matrix produces higher plastic deformation than soft inclusions in the hard matrix but stresses are higher for soft inclusions in the hard matrix than for soft inclusions in the hard matrix along with plastic deformation.

Keywords: *hard/soft inclusions; hard/soft matrix; finite element simulation; plastic deformation*

1. Introduction

Hard inclusions embedded in the soft matrix are a basic building principle of metal matrix composites (MMCs) [1], [2] particle reinforced metal matrix composites (PRMCs) [3] or metal matrix nanocomposites (MMNCs) [4]. Generally, hard inclusions in the soft matrix have function as a strength load bearer and the soft (ductile) matrix primarily distributes and transfers load [5]. Soft inclusions in the hard matrix can be found in cementitious composites [6], [7], plastics like acrylonitrile-butadiene-styrene (ABS) [8] or soil [9]. Soft inclusions in the hard matrix reduce strength [6] [8] [9] but increase toughness [10] [11] [12].

Finite element (FE) simulations have been widely used to study mechanical behaviour of inclusions in matrix [3] [13] [14] [15] [16] [17] [18]. Two methods are usually employed in FE simulations. Firstly, the representative volume element (RVE) [14] [17] is used. RVE has drawback in necessity to conduct homogenisation firstly in order to estimate an elastic properties of the regarded volume [13] [19] and there is a restriction of the method in conjunction with plastic deformation (not existed solution for softening materials) [19]. Secondly, the "micromechanical model" can be represented by spherical, triangle, square or random shape of the inclusions [16]. In [18] was shown that computed stress on the inclusion and on the interface inclusion-matrix is very well predicted by FE simulation (in comparison with theory and in exception of polygonal inclusion) but that paper is devoted to the one isolated inclusion and linear elasticity.

According to the author experience, the effect of inclusions in matrix and generally micromechanical aspects are relatively complicated implemented into the industrial FE simulations. For instance, implementing (short reinforced) plastic injection moulding simulation requires exporting the moulding data which requires usually a buying an additional software module; importing the moulding data to structural FE simulations requires additional software (module). Furthermore, the material model for the structural FE simulations has to be built on the moulded data – additional software (the situation with metal injection moulding is even more complicated due to the debinding and sintering and will not be described). Therefore, the study of the

* Corresponding author: Michal Kráčalik, E-mail address: michal.kracalik@gmail.com

effect of the inclusions on the stress distribution and plastic deformation using a traditional continuum mechanical FE simulation approach can be interesting from the practical point of view. Such approach will miss detail information about the inclusions distribution and their local effect on the stress and plastic deformation but gives and orientation value that can be implemented into the safety factors.

The aim of this paper is investigation of stress and strain behaviour of hard/soft inclusions embedded in the hard/soft matrix using FE simulations. 1% and 2% inclusion volume fraction is assumed in the 2-D plain strain FE model assuming elastic-plastic material model. Additionally, the diameter and the number of the circular inclusions are varied and Equivalent von-Mises Stress and (further as "Mises stress") and Equivalent plastic strain (further as "PEEQ") are evaluated.

2. FE and Material model

2-D plane strain finite element (FE) model consists of square part with size of $100 \times 100 \mu\text{m}$. The thickness of the model is $100 \mu\text{m}$. Hard and soft inclusions are embedded in the hard or soft matrix as is shown in Figure 1. Inclusions are distributed in the FE model. A uniform distribution is created by Python's library "numpy" with the function "random.rand" and positions of inclusions are imported to FE software Ansys. The number and size of the inclusions are chosen to produce 1% and 2% inclusion volume fraction in the FE model. Assumed is circular shape of the inclusions with diameter d approximately equal to $3.57 \mu\text{m}$ and $5.05 \mu\text{m}$. Ten and twenty inclusions are embedded in the matrix with bonded contact prescribed between inclusions and the matrix. Mesh element size is $1 \mu\text{m}$. FE model is loaded with tensile loading of 300 MPa at the top edge and fixed at the bottom edge, see Figure 1.

The material model is based on the crystal plasticity calculations conducted in [20]. There were studied mechanical behaviour of dual-phase steel DP800. DP800 and separated ferrite and martensite true stress-strain curves were presented in the referenced paper [20]. Ferrite and martensite curves are presented in Figure 2 as they are modeled with multilinear isotropic hardening material model in Ansys. Ferrite represents soft inclusion or matrix and martensite represents hard inclusion or matrix in

this paper.

While current paper is neither devoted to steel DP800 nor crystal plasticity calculations, reader is referred for more information to free available paper [20].

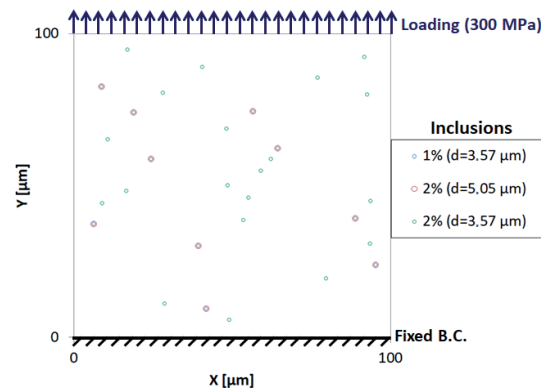


Figure 1: Scheme of the FE model. Modelled circular shaped inclusions are uniformly distributed in the FE model with approximate diameters of $3.57 \mu\text{m}$ and $5.05 \mu\text{m}$ in order to produce 1% and 2% inclusion volume fraction. Ten and twenty inclusions are embedded in the FE model.

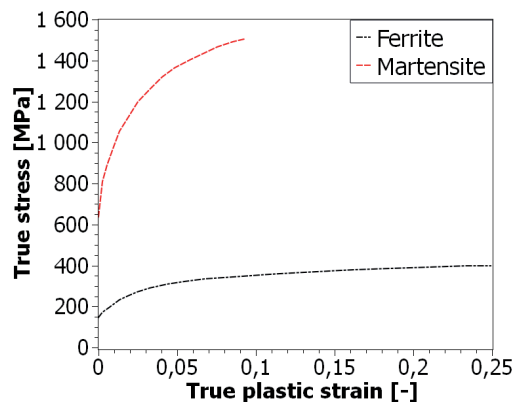


Figure 2: True stress-plastic strain curves (multilinear isotropic hardening material model in Ansys) of ferrite and martensite based on the crystal plasticity calculation presented in [20]. Ferrite will represent soft inclusion or matrix and martensite hard inclusion or matrix further in the paper.

3. Results and Discussion

Figures 3a and 3b show Mises Stress. Figure 3a shows hard inclusions in the soft matrix and Figure 3b shows soft inclusions in hard matrix. Figure 3b contains additionally detail on one inclusion. Equivalent Plastic Strain PEEQ is shown in Figure 3c and 3d. Figure 3c shows hard inclusions in the soft matrix Figure 3d shows soft inclusions in the hard

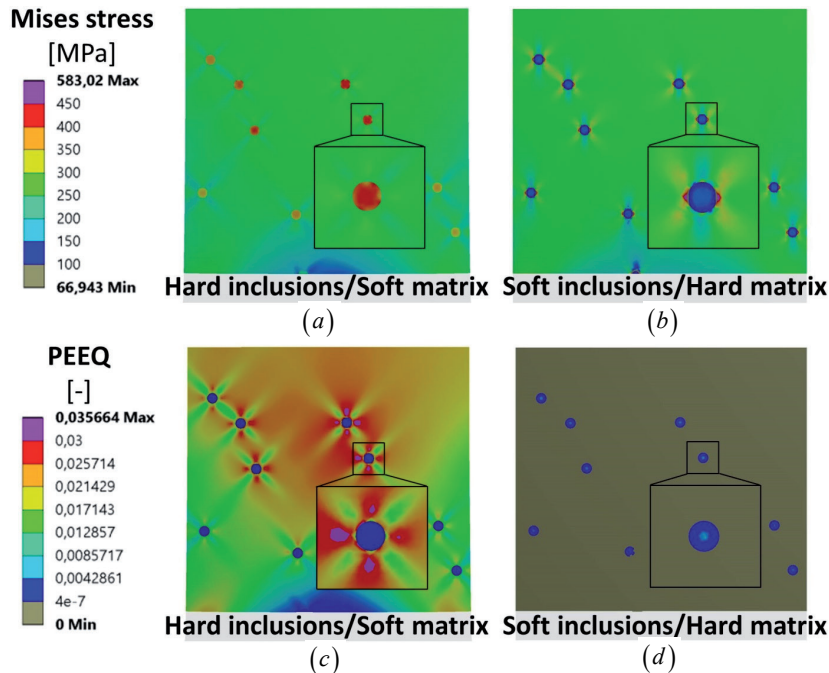


Figure 3: (a) Mises stress: hard inclusions in the soft matrix. (b) Mises stress with: soft inclusions in the hard matrix (with detail on the stress distribution around the inclusion). (c) Equivalent Plastic Strain (PEEQ): hard inclusions in the soft matrix. (d) PEEQ soft inclusions in the hard matrix (very small PEEQ is calculated – the maximum is 0.00080584). 1% inclusions with diameter $d=3.57\ \mu\text{m}$ is depicted in Figure 3. Ten inclusions are embedded in the matrix.

matrix. 1% percent inclusions in the matrix is shown in Figure 3 (ten inclusions with approximately diameter $d=3.57\ \mu\text{m}$). Lower $10\ \mu\text{m}$ are excluded from the analysis – due to the high deformation of the soft matrix, high plastic deformation is computed nearby the boundary condition on the corner between horizontal (x-axis) and vertical (y-axis) edges of the FE Model. However, it can be shown that such boundary condition effect influences the results negligible but the exclusion of the lower part from the analysis helps significantly with the displaying of the computed results.

Higher Mises stress is calculated on hard inclusions embedded in the soft matrix that on soft inclusions embedded in hard matrix, see Figures 3a and 3b. The highest Mises stress (approximately 583 MPa) is calculated at the hard matrix just at the bonded contact with soft inclusion in the perpendicular direction on the acted loading, see Figure 3b.

The highest PEEQ is calculated on soft matrix at the bonded contact with the hard inclusion that is located nearest to the right upper corner, Figure 3c. High PEEQ is always calculated in the

perpendicular x-y directions, Figure 3c. PEEQ raises from the boundary condition at the bottom of the FE model to the top edge of the FE model where the loading acts, Figure 3c. Practically no PEEQ (maximum 0.00080584) is calculated for soft inclusions embedded in the hard matrix, Figure 3d.

Using a soft matrix, material can flow around hard inclusions and PEEQ is calculated in the soft matrix, Figure 3c. Mises stresses are smaller in the soft matrix than in inclusions but the soft matrix poses small yield strength about 145 MPa (see Figure 2) and is plastically deformed, Figure 3a, 3c. On the other hand, relatively high Mises stresses lying between 430–470 MPa does not enforce yielding of hard inclusions due to the high yield strength around 638 MPa, see Figure 3a, 3c and 2. High Mises stresses at the hard inclusions are caused by the reaction against the irreversible material motion of the soft matrix.

Using a hard matrix, soft inclusions are stretched in the loading direction and the hard matrix reacts with high Mises stresses because of assumed the bonded contact between inclusions and the matrix, see depicted detail in Figure 3b. While hard matrix

does not allow to stretch the inclusions, very small PEEQ is calculated, Figure 3d.

Figure 4 shows a summary of the computed results. Figure 4a shows the maximum Mises stress and Figure 4b shows the maximum PEEQ. For ferrite and martensite (FE models without inclusions) are calculated approximately same Mises stress, see Figure 3a. The reason is the prescribed load in the FE model. PEEQ differs significantly between ferrite and martensite; martensite demonstrates zero PEEQ while ferrite demonstrates noticeable PEEQ, Figure 4b. This results follow the true stress-true plastic strain curves (material model) shown in Figure 2.

Soft inclusions in the hard matrix produce small PEEQ but the Mises stresses are high in comparison with hard inclusions in the soft matrix, Figure 4a. Hard inclusions in the soft matrix cause high PEEQ and smaller Mises stresses than soft inclusions in the hard matrix, Figure 4b.

Using the approximately inclusion diameter $d=3.57\ \mu\text{m}$, 2% inclusion volume fraction (20 inclusions) produces higher Mises stress as well as higher PEEQ than 1% inclusion volume fraction (10 inclusions) for both inclusions/matrix variations, Figure 4. 2% inclusion volume fraction with 20 inclusions ($d=3.57\ \mu\text{m}$) produces higher Mises stresses than 2% inclusion volume fraction with 10 inclusions ($d=5.05\ \mu\text{m}$), Figure 4a. It is not the case for PEEQ, Figure 4b. Hard inclusions in the soft matrix with 20 inclusions (2%; $d=3.57\ \mu\text{m}$) gives smaller PEEQ than hard inclusions in the soft matrix with 10 inclusions (2%; $d=5.05\ \mu\text{m}$). The reason has a numerical character. The highest calculated PEEQ is normally located around the same inclusion as the highest calculated Mises stress due to the action-reaction rule (see text above Figure 3) but here, the action-reaction rule has been broken due to sensitive contact calculation. Same numerical problem can be drawn for 10 soft inclusions (2%; $d=5.05\ \mu\text{m}$) where the maximum PEEQ and Mises stress are slightly lower than for 10 Soft inclusions (1%; $d=3.57\ \mu\text{m}$). However, taking into account numerical issue, following trends can be assumed: Firstly, 2% inclusions produce higher PEEQ and Mises stress than 1% inclusions. Secondly, 2% inclusions with diameter $d=3.57\ \mu\text{m}$ (20 inclusions) produce more PEEQ and Mises stress than 2% inclusions with diameter $d=5.05\ \mu\text{m}$ (10 inclusions).

The computed PEEQ (Figure 3c, 3d) has been compared with the literature [16]. Computed results

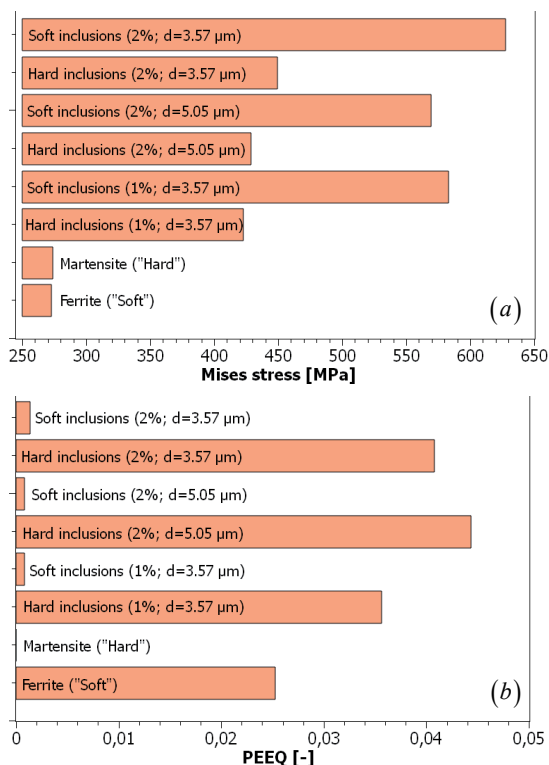


Figure 4: (a) The maximum Mises stress in the FE model. (b) The maximum Equivalent Plastic strain (PEEQ) in the FE model. Soft inclusions mean soft inclusions in the hard matrix (ferrite inclusions in the martensite matrix) and hard inclusions mean hard inclusions in the soft matrix (martensite inclusions in the ferrite matrix) in Figure 4. 2% inclusions with diameter $d=3.57\ \mu\text{m}$ consist of 20 inclusions and with diameter $d=5.05\ \mu\text{m}$ consist of 10 inclusions. 1% inclusions with diameter $d=3.57\ \mu\text{m}$ consist of 10 inclusions.

correspond with the literature – hard inclusions in the soft matrix cause PEEQ outside the inclusions while soft inclusions in the hard matrix cause PEEQ in the inclusions, Figure 3c, 3d; FE model is supposed to be verified; however, stresses are not shown in [16].

Martensite ("Hard") and ferrite ("Soft") phases are based on the crystal plasticity simulation of the dual-phase steel DP800 conducted in [20]. Martensite volume fraction is 46% and ferrite volume fraction is 54% in DP800 but in this paper is used 1% and 2% for both phases, respectively. This work does not reconstruct the mechanical behaviour of the DP800 as is for instance (for similar dual-phase steel DP780) done in [21]. Therefore, the used material model should be viewed only as a hard and soft phase

regardless its origin in this paper.

4. Conclusions

FE study investigates the effect of the hard/soft inclusions embedded in the hard/soft matrix. The material model of the hard and soft phases is based on the martensite and ferrite true stress-strain curves taken from the literature. Inclusions increase Mises stress in the FE model but only hard inclusions in the soft matrix cause high equivalent plastic strain. On the other hand, soft inclusions reduce equivalent plastic strain in spite of high Mises stresses. FE model is verified and results are discussed in the paper.

A simple approach presented in the paper can help estimate an effect of the inclusions in the matrix on the mechanical stresses (plastic deformation) in the praxis without performing additional processing simulations. For instance, presented maximal Mises stresses are almost twice high than a nominal Mises stresses (outside the inclusion influenced region). However, practical applicability has to be regarded to specific material classes like metals, engineering plastics, ceramics and ceramics composites, concrete and rocks including their processing route, their geometry and loading conditions.

Because the interface between the matrix and inclusions is stiff, the next step in the research can be comparison of some interface properties.

References

1. B. Ji, H. Gao, and T. Wang, "Flow stress of biomorphous metal-matrix composites," *Materials Science and Engineering: A*, vol. 386, pp. 435-441, 2004. [Online]. <http://www.sciencedirect.com/science/article/pii/S0921509304010007>
2. B. McWilliams, J. Yu, E. Klier, and C.-F. Yen, "Mechanical response of discontinuous ceramic fiber reinforced metal matrix composites under quasi-static and dynamic loadings," *Materials Science and Engineering: A*, vol. 590, pp. 21-29, 2014. [Online]. <http://www.sciencedirect.com/science/article/pii/S0921509313010538>
3. R. Ekici, M. K. Apalak, M. Yildirim, and F. Nair, "Simulated and actual micro-structure models on the indentation behaviors of particle reinforced metal matrix composites," *Materials Science and Engineering: A*, vol. 606, pp. 290-298, 2014. [Online]. <http://www.sciencedirect.com/science/article/pii/S092150931400344X>
4. M. U. Siddiqui, A. F. M. Arif, Saheb Nouari, and M. Shahzeb Khan, "Constitutive modeling of elastoplasticity in spark-plasma sintered metal-matrix nanocomposites," *Materials Science and Engineering: A*, vol. 689, pp. 176-188, 2017. [Online]. <http://www.sciencedirect.com/science/article/pii/S0921509317302083>
5. J. Zhang et al., "In situ synchrotron high-energy X-ray diffraction study of microscopic deformation behavior of a hard-soft dual phase composite containing phase transforming matrix," *Acta Materialia*, vol. 130, pp. 297-309, 2017. [Online]. <http://www.sciencedirect.com/science/article/pii/S1359645417302471>
6. G. Falzone et al., "The influences of soft and stiff inclusions on the mechanical properties of cementitious composites," *Cement and Concrete Composites*, vol. 71, pp. 153-165, 2016. [Online]. <http://www.sciencedirect.com/science/article/pii/S095894651630141X>
7. Z. Wei et al., "Restrained shrinkage cracking of cementitious composites containing soft PCM inclusions: A paste (matrix) controlled response," *Materials & Design*, vol. 132, pp. 367-374, 2017. [Online]. <http://www.sciencedirect.com/science/article/pii/S026412751730655X>
8. Sen Zhang et al., "Toughening plastics by crack growth inhibition through unidirectionally deformed soft inclusions," *Polymer*, vol. 54, pp. 6019-6025, 2013. [Online]. <http://www.sciencedirect.com/science/article/pii/S0032386113007957>
9. G. Van Lysebetten, A. Vervoort, J. Maertens, and N. Huybrechts, "Discrete element modeling for the study of the effect of soft inclusions on the behavior of soil mix material," *Computers and Geotechnics*, vol. 55, pp. 342-351, 2014. [Online]. <http://www.sciencedirect.com/science/article/pii/S0266352X13001596>
10. S. A. Ngah and A. C. Taylor, "Toughening performance of glass fibre composites with core-shell rubber and silica nanoparticle modified matrices," *Composites Part A: Applied Science and Manufacturing*, vol. 80, pp. 292-303, 2016. [Online]. <http://www.sciencedirect.com/science/article/pii/S1359835X15003929>
11. L. Ruiz-Pérez, G. J. Royston, J. P. A. Fairclough, and A. J. Ryan, "Toughening by nanostructure," *Polymer*, vol. 49, pp. 4475-4488, 2008. [Online]. <http://www.sciencedirect.com/science/article/pii/S003238610800579X>
12. Y. Jiang, "Micromechanics constitutive model for predicting the stress-strain relations of particle toughened bulk metallic glass matrix composites," *Intermetallics*, vol. 90, pp. 147-151, 2017. [Online]. <http://www.sciencedirect.com/science/article/pii/S0966979517305174>
13. J. Li, E. Martin, D. Leguillon, and C. Dupin, "A finite fracture model for the analysis of multi-cracking in woven ceramic matrix composites," *Composites Part B: Engineering*, vol. 139, pp. 75-83, 2018. [Online]. <http://www.sciencedirect.com/science/article/pii/S1359836817306777>
14. Y. Solyaev and S. Lurie, "Numerical predictions for the

- effective size-dependent properties of piezoelectric composites with spherical inclusions," *Composite Structures*, vol. 202, pp. 1099-1108, 2018, Special issue dedicated to Ian Marshall. [Online]. <http://www.sciencedirect.com/science/article/pii/S0263822318301971>
15. U. Santhosh, J. Ahmad, G. Ojard, R. Miller, and Y. Gawayed, "Deformation and damage modeling of ceramic matrix composites under multiaxial stresses," *Composites Part B: Engineering*, vol. 90, pp. 97-106, 2016. [Online]. <http://www.sciencedirect.com/science/article/pii/S1359836815007520>
 16. A. Gupta, A. Cecen, S. Goyal, A. K. Singh, and S. R. Kalidindi, "Structure-property linkages using a data science approach: Application to a non-metallic inclusion/steel composite system," *Acta Materialia*, vol. 91, pp. 239-254, 2015. [Online]. <http://www.sciencedirect.com/science/article/pii/S1359645415001603>
 17. S. Ghosh and S. Moorthy, "Particle fracture simulation in non-uniform microstructures of metal-matrix composites," *Acta Materialia*, vol. 46, pp. 965-982, 1998. [Online]. <http://www.sciencedirect.com/science/article/pii/S1359645497002899>
 18. Y. Nakasone, H. Nishiyama, and T. Nojiri, "Numerical equivalent inclusion method: a new computational method for analyzing stress fields in and around inclusions of various shapes," *Materials Science and Engineering: A*, vol. 285, pp. 229-238, 2000. [Online]. <http://www.sciencedirect.com/science/article/pii/S0921509300006377>
 19. H. Askes and E. C. Aifantis, "Gradient elasticity in statics and dynamics: An overview of formulations, length scale identification procedures, finite element implementations and new results," *International Journal of Solids and Structures*, vol. 48, pp. 1962-1990, 2011. [Online]. <http://www.sciencedirect.com/science/article/pii/S0020768311001028>
 20. Y. Xu, W. Dan, C. Ren, T. Huang, and W. Zhang, "Study of the Mechanical Behavior of Dual-Phase Steel Based on Crystal Plasticity Modeling Considering Strain Partitioning," *Metals*, vol. 8, 2018. [Online]. <http://www.mdpi.com/2075-4701/8/10/782>
 21. S. Huang et al., "Uniaxial Tension Simulation Using Real Microstructure-based Representative Volume Elements Model of Dual Phase Steel Plate," *Procedia Engineering*, vol. 81, pp. 1384-1389, 2014, 11th International Conference on Technology of Plasticity, ICTP 2014, 19-24 October 2014, Nagoya Congress Center, Nagoya, Japan. [Online]. <http://www.sciencedirect.com/science/article/pii/S1877705814014404>

